Chemical structure and adhesion of DLC film with amorphous SiC interlayer

†*Xia Zhu[1], Hiromichi Toyota[1], Daiki Muranaka[1],

Yutaroh Kimura[1] and Ryoya Shiraishi[1]

[1]Department of Mechanical Engineering, Faculty of Engineering, Ehime University, JP

*Presenting author: zhu.xia.mx@ehime-u.ac.jp
†Corresponding author: zhu.xia.mx@ehime-u.ac.jp

Abstract

This study was performed to improve the adhesiveness of a diamond-like carbon (DLC, a-C:H) multilayer film with an a-SiC interlayer. DLC (a-C: H) multilayer film with an a-SiC interlayer were deposited, and residual stresses the influence of the residual stresses on the adhesion of the film were investigated. The following conclusions can be drawn from the results presented herein: first, the a-SiC interlayer affects the DLC film structure. When the thickness of the interlayer t <= 0.25 m μm, the proportion of sp 3 bonds in the DLC film is approximately constant and about 10%. In the case of t> 0.25 μm, the proportion of sp3 bonds in the DLC film tends to decrease slightly. Second residual compressive stress exists in the DLC film, but residual tensile stress or compressive residual shrinkage stress exists in the a-SiC interlayer. Third, the residual stress of the DLC film is not due to the peeling failure of the film. Fourth, the residual tensile stress of the a-SiC interlayer does not cause the peeling failure of the film, but a part of the compressive residual stress causes the local buckling of the interlayer film and may also cause the peeling failure of the film. Finally, the strength and rigidity of the a-SiC interlayer dominate the adhesion between the a-SiC-DLC multilayer film and the substrate.

Keywords: Diamond-like carbon film, Amorphous silicon carbide interlayer, Raman spectral analysis, I (D) / I (G) ratio, FWHM (G), residual stress

Introduction

Diamond-like carbon (DLC) is an amorphous carbon material containing a mixture of sp2 hybridized graphite, and sp3 hybridized diamond. DLC exhibits good abrasion resistance and high chemical safety due to its diamond content and flatness/low counterbody aggressiveness due to the presence of graphite. Thus, DLC is expected to be useful as a coating material [1]. However, a large obstacle for applications of DLC film is its low adhesiveness to various substrates, which is caused by two main factors: intrinsic residual stress and stable carbon bonds [2]. Several reports [3] have detailed attempts to prevent layer separation and improve the adhesiveness of DLC thin layers by forming an interlayer of silicon carbide (SiC) with high substrate adhesiveness, and then covering the interlayer with the DLC. However, uncertainties remain regarding the optimal conditions for forming a SiC thin film and DLC/a-SiC stacked thin layer. In particular, no reports have been published to date regarding the effects of an a-SiC thin film on the structure and film thickness. The goal of this study is to improve the adhesiveness of a DLC/a-SiC layered film formed by ion plating. In previous studies, the formation of a hydrogen-containing DLC (a-C: H) /a-SiC layered thin film was achieved, and the effects of an a-SiC interlayer on its structure and mechanical properties were determined.

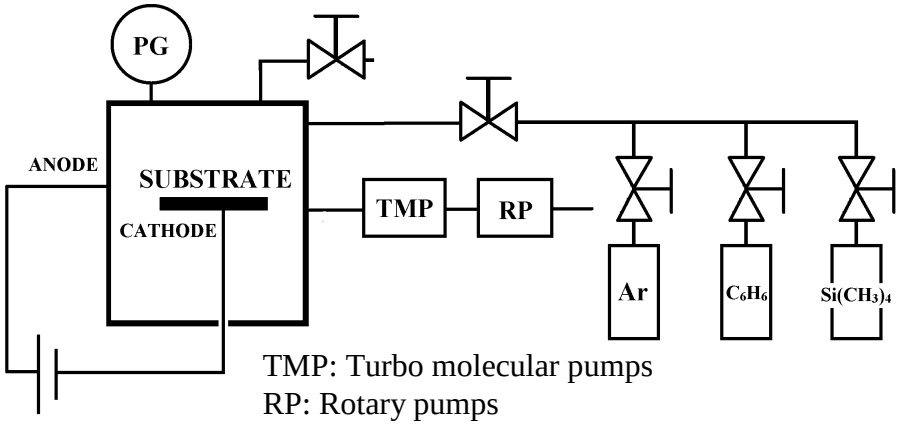

Fig. 1 Schematic diagram of the experimental setup for the ion plating method with introduction of reactive gas

Film Deposition and Evaluation Methods

Experimental Apparatus for Film Deposition and Evaluation Methods

The ion plating methodwas used to form the a-SiC interlayer and DLC/a-SiC stacked layer. A schematic of the experimental apparatus is shown in Fig. 1, consisting of a vacuum chamber, rotary pump, turbo molecular pump, high-voltage power device, gas supply system, negative electrode substrate, and positive electrode chamber inner wall. Using rotary and turbo molecular pumps, it was possible to reduce the pressure in the chamber to 1.0 x 10-3 Pa. We built a power device consisting of a variable pressure system/bridge rectifying circuit that was capable of outputting a maximum of 500 V. The gas supply system could supply argon (Ar), benzene (C6H6), and tetramethylsilane (TMS, Si (CH3)4).
A stainless steel SUS304 (JIS G 4304, width 10 x length 30 x thickness 1.5 mm) substrate was pulverized and ultrasonically cleaned in an acetone solution. Subsequently, the substrate was fastened inside the chamber and the pressure inside the chamber was reduced using rotary and turbo molecular pumps. Inert gas was introduced into the chamber and the pressure adjusted. Voltage was applied to turn the inert gas into plasma and the substrate was washed by sputtering. To form the Si-C layer, tetramethylsilane was introduced into the chamber, turned to plasma, and deposited onto the substrate as an interlayer. For the DLC layer, benzene was introduced into the chamber, turned into plasma, and deposited on the substrate.
In this experiment, argon/TMS (mixing ratio of 1:1) gas was introduced, an interlayer was formed for 0 to 3 min, and a-SiC films 0.05 to 0.45 μm in thickness were formed. Subsequently, argon and benzene (mixing ratio of 1:1) were introduced, and a DLC film with a thickness of 2 μm was formed in 30 min.

Chemical Structure Analysis on film

Visible Raman spectral analysis is effective for analyzing the structure of DLC films [4-10]. Typical Raman spectra were observed for the prepared DLC when as shown in Fig. 2 [11]. From Fig. 2, the Raman spectrum of the DLC film could be divided into a D peak near 1350 cm-1 arising from the stretching and contracting of the six membered ring, and a G peak between 1500 and 1600 cm^{-1} originating from the vibrations of the sp2 carbons on the chain and ring. The G-peak position and the FWHM (G) were used as parameters to qualitatively evaluate the degree of amorphous nature of the film (or crystallization). In addition, the hydrogen density of the film was evaluated using the photoluminescence (PL) of the Raman

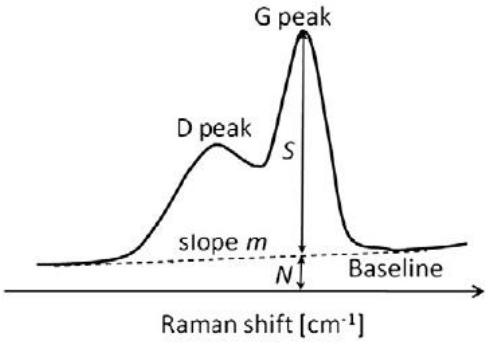

Fig. 2 Raman peak obtained for the DLC film [11]

curve. The baseline slope m [8] of the Raman spectrum and the ratio (log N/S) [9] of the photoluminescence component N to the strength of the Raman scattering at the G peak position were used as Raman parameters. In this study, a Raman spectrometer was used to evaluate the structure of the film with an oscillating Ar ion laser (514 nm), laser output of 1.0 mW, and an analysis range of 20 μm Φ.

Calculation of residual stress in film

The average residual stress σ_i of a film can be calculated from the curvature of the substrate (substrate deformation method), that is, the radius of curvature using the following Stoney equation (1) [12].

$$\sigma_i = -\frac{E_s t_s^2}{3(1-\nu_s)t_F} \cdot \frac{1}{R} \tag{1}$$

Where, E s and ν s are the Young's modulus and Poisson's ratio of the substrate, t s and t F are the substrate thickness and thin film thickness, respectively, and R is the curvature radius of substrate warpage. The residual stress can be determined by measuring the curvature R of the specimen on which DLC is deposited. Here, assuming that the substrate has a convex shape upward, the curvature of the R is defined as positive, and the negative σ_i indicates that the residual stress is a compressive stress. In order to measure R, a contact-type surface roughness tester was used.

In this research, the DLC film deposited is a film of two layers from the a-SiC intermediate layer and the DLC film, and the formula (1) cannot calculate the residual stress of each layer. Therefore, the residual stress was calculated using the residual stress calculation equation (2) corresponding to the film of the two-layer structure proposed by Nakamura et al. [13].

$$\sigma_F = \sigma_i \cdot \frac{t_i}{t_F} - \frac{E_S t_s^2}{3(1-\nu_s)t_F} \cdot \frac{1}{R} \tag{2}$$

where, σ_i is a residual stress of the intermediate layer, and σ_F is a residual stress of the outermost layer. Therefore, the residual stress of the intermediate layer can be calculated by equation (1), the radius of curvature of the substrate of the thin film having a two-layer structure can be measured, and the residual stress of the outermost layer can be calculated using equation (2). In the case of the test piece with only the a-SiC intermediate layer, there was a case that it

did not have a clear arc shape because the deformation of the substrate was partially waved. The stress value was set to zero for such specimens.

Evaluation of adhesion between film and substrate

During the film deposition, a residual stress generated inside the film reduces the adhesion between the film and the substrate, and in some cases, the film peels off the substrate. In this study, the adverse effect of the residual tensile stress on film adhesion is evaluated by a stress intensity factor. On the other hand, the adverse effect of the compressive residual stress is evaluated by a buckling load. Assuming that the mode of a crack surface displacement due to tensile residual stress is the opening mode, the stress intensity factor K_I is expressed by equation (3) [14].

$$K_{\mathrm{I}} = \sigma \sqrt{\pi a} \tag{3}$$

where, σ is an average stress in the film, and a is a length of the latent crack in the film.
In the a-SiC intermediate layer, it is an internal penetration crack with the length $a = 1 / 2t_{a\text{-}SiC}$, and in the DLC film, it is a surface penetration crack with the length $a = t_{DLC}$. If the stress intensity factor is large, the risk of film peeling due to crack growth due to the tensile stress increases. On the other hand, even if a compressive stress is applied to the crack surface, crack propagation does not occur, so the stress intensity factor in that case is set to zero. However, the compressive stress may cause the film to buckle and also cause the film to peel off the substrate.
The Euler buckling load Pc of a beam fixed at both ends is expressed by the equation (4) [15].

$$P_{\mathrm{c}} = \frac{4\pi^2 EI}{l^2} \tag{4}$$

Where, E is an elasticity modulus, I is a second moment of area, and l is a length of the beam. In this study, the elastic modulus of a-SiC interlayer and DLC film were set to 80 GPa and 100 GPa, respectively. In addition, l was 10 μm in consideration of the surface roughness of the substrate. As the compressive load on the cross section of the film due to residual the compressive stress approaches the Euler buckling load, buckling of the film is more likely to occur.

Results and Discussion

Changes in chemical structure

Generally, it is possible to gain information regarding the structure of the film and chemical bonding of the carbon atoms from the position of the G-band, the behavior of the I (D)/I (G), and FWHM(G), which can be obtained from the results of the Raman spectrum. Ferrari et al. [6] developed a model wherein upon introduction of defects into graphite to create disorder, an amorphization trajectory can be classified into three stages according to strength (Fig. 3). Specifically, from the monocrystalline to nanocrystal graphite, this model describes the series of disordering processes, with a third stage leading to the formation of tetrahedral amorphous carbon (ta-C) with sp^3 bonding, via amorphous carbon (a-C), which contains mainly sp^2 bonds. These structural and chemical bonding state changes can be observed in the visible (514 nm) Raman spectrum. The G-peak is a parameter depends on the length of the sp^2 bonds between the carbon atoms in the DLC film, and shifts to higher frequencies as the bond lengths shorten.

Therefore, the DLC film where the G-peak is located at high frequency indicates a higher degree of graphite crystallization. In contrast, the FWHM (G) indicates the degree of amorphous character of the graphite. When various bond lengths exist, as in DLC films with marked amorphous character, the G peak appears over a broad range. Therefore, the G peak becomes broadens for the DLC film overall, and, as a result, the FWHM (G) increases. The G peak position shifts to higher frequencies as the amorphous character of the film increases. Generally,

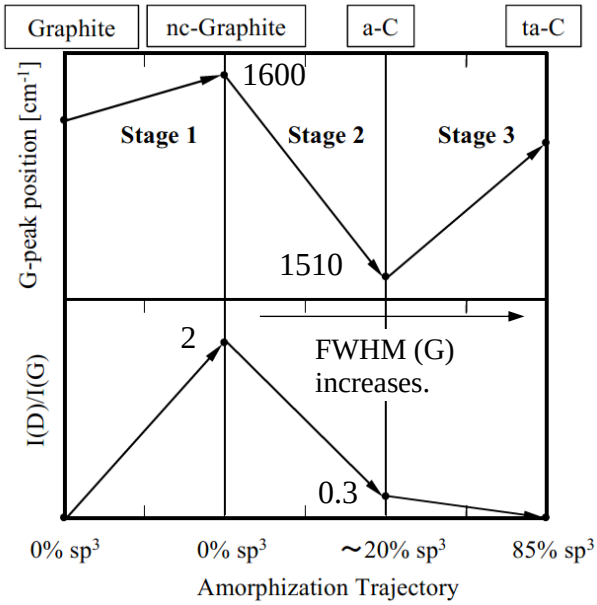

Fig. 3 Amorphization trajectory, showing a schematic variation of the G peak position, *I*(D)/*I*(G) ratio and *FWHM* (G) [6]

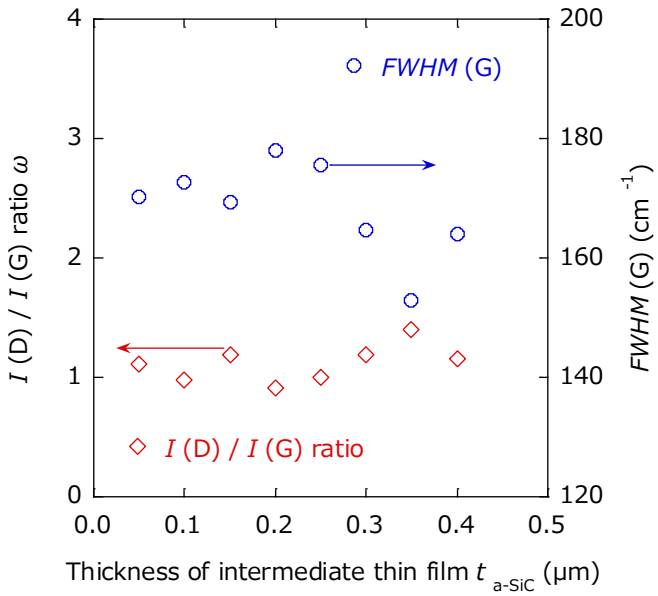

Fig. 4 *I* (D) / *I* (G) ratio and *FWHM* (G) for each interlayer thickness

amorphous films contain a high degree of sp3 bonds, which is positively correlated with FWHM (G) and hardness [7]. This model of structural changes from stages 1 to 3 shown in Fig. 3 was studied by correlation with the Raman spectra of the DLC films.
Figs. 4 and 5 respectively show I (D) / I (G) ratio, FWHM (G) and Raman shift at G peak position values for each interlayer thickness. When the intermediate layer is thin (t <= 0.25), I (D) / I (G), FWHM (G) and Raman shifts ω at G peak positions are almost constant, with some variations. As the intermediate layer becomes thicker, it tends to increase in I (D) / I (G) and

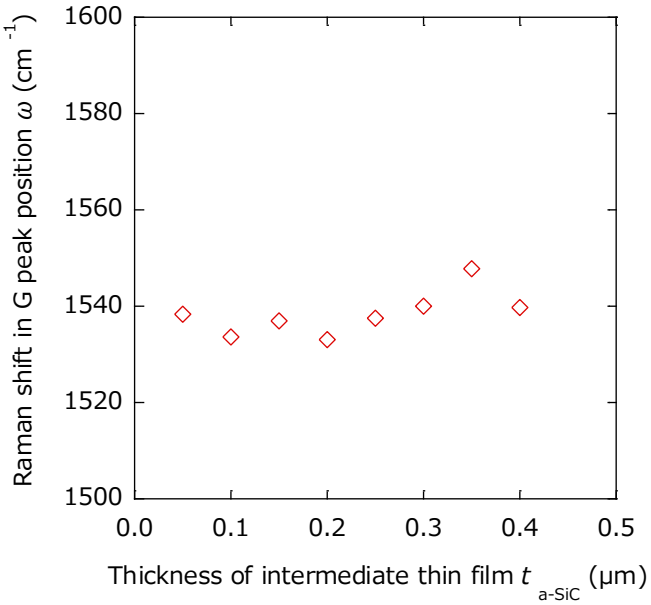

Fig. 5 Raman shift in G peak position for each interlayer thickness

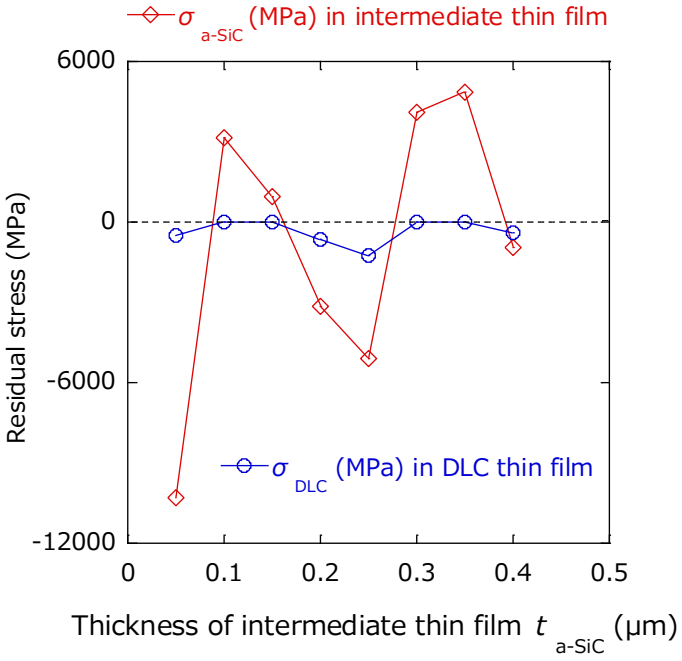

Fig. 6 Changes of residual stress in a-SiC intermediate film and DLC film.

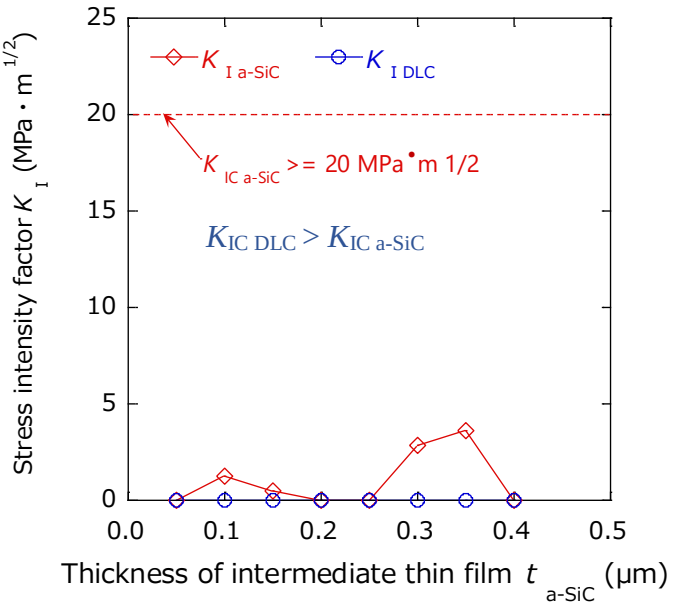

Fig. 7 Changes of residual stress in a-SiC intermediate film and DLC film

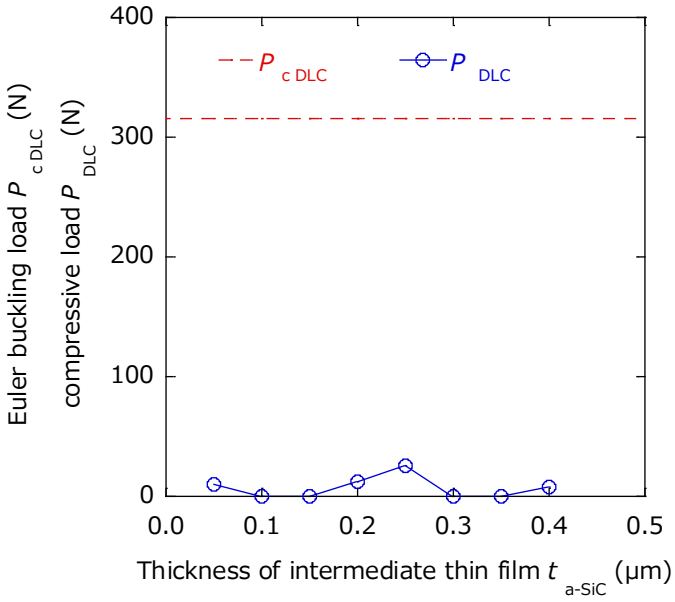

Fig. 8 Euler buckling loads and compressive loads in DLC film

Raman shifts ω, but decreases in FWHM (G). Compared to FIG. 3, the proportion of sp3 bonds in the DLC film is approximately 10%.

Changes in residual stress in a-SiC fime and DLC film

Fig.6 shows the residual stress σ a-SiC in the a-SiC thin film and the residual stress σ DLC in the DLC thin film by the intermediate layer thickness. In any thickness of the a-SiC interlayer, the intermediate thin film had a considerably higher residual stress than the DLC thin film.
The stress intensity factor in the residual stress field is shown in Fig.7. Since no tensile stress is applied to the DLC film, the stress intensity factor is zero. Therefore, even if there is a latent

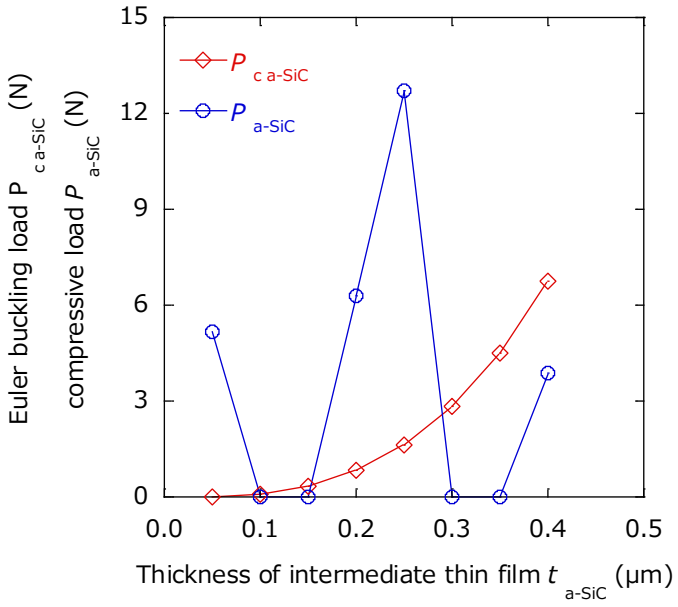

Fig. 9 Euler buckling loads and compressive loads in a-SiC film

surface penetration crack of the DLC film, the crack does not become the origin of the peel fracture of the film. On the other hand, although the a-SiC intermediate thin film has a larger tensile stress than the DLC film, the maximum stress intensity factor does not exceed the fracture toughness value, so even if there is a latent penetration crack in the film, the crack does not progress.

Figures 8 and 9 show the Euler buckling load and compressive residual stress of both films applied to the cross section of the film. In the case of a DLC film, no buckling occurs because the compressive load due to residual stress is much smaller than the buckling load.

On the other hand, at t a-SiC = 0.05, 0.2, 0.25, 0.4 μm, compressive residual stress is applied to the a-SiC intermediate thin film, and local buckling of the film does not occur only at t = 0.4 μm, and in other cases, local buckling of the membrane occurs.

In the experimental results of film depositions, peeling failure of the film was confirmed only at t = 0.05 μm. From the results, in the case of t = 0.05, the buckling of the whole film was caused by the local buckling of the interlayer. On the other hand, in the case of t = 0.2 and 0.25, local buckling occurred in the film but it did not reach the entire film.

From the above, the strength and rigidity of the a-SiC interlayer greatly affect the adhesion of the multilayer film than the DLC film. The reduction of the residual stress of the a-SiC interlayer can improve the film adhesion.

In the future, using quantum chemical calculation program Gaussian and finite element method program MSC. Marc, we will investigate the mechanism of interfacial peeling failure of the film and find the optimum deposition conditions for improving the adhesion of the film.

Conclusion

DLC (a-C: H) multilayer film with an a-SiC interlayer were deposited, and residual stresses the influence of the residual stresses on the adhesion of the film were investigated. The following conclusions can be drawn from the results presented herein:

(1) The thickness of the a-SiC interlayer affects the DLC film structure. When the thickness of the interlayer $t_{a\text{-}SiC}$ <= 0.25 m μm, the proportion of sp 3 bonds in the DLC film is approximately

constant and about 10%. In the case of $t_{a\text{-}SiC} > 0.25$ μm, the proportion of sp3 bonds in the DLC film tends to decrease slightly.

(2) In the film deposition process, residual compressive stress exists in the DLC film, but residual tensile stress or compressive residual shrinkage stress exists in the a-SiC interlayer.

(3) The residual stress of the DLC film is not due to the peeling failure of the film.

(4) The residual tensile stress of the a-SiC interlayer does not cause the peeling failure of the film, but a part of the compressive residual stress causes the local buckling of the interlayer film and may also cause the peeling failure of the film.

(5) The strength and rigidity of the a-SiC interlayer dominate the adhesion between the a-SiC-DLC multilayer film and the substrate.

References

[1] J. Robertson, (1992) Properties of Diamond-Like Carbon, Surf. Coat. Technol. **50**, 185-195.

[2] K. Akari, (2002) Improvement in Adhesion of DLC Coating, J. Japanese Soc. Tribol. **47**, 809-814.

[3] Z. Sun, C. H. Lin, Y. L. Lee, J. R. Shi, B. K. Tay and X. Shi, (2000) Effectsn on deposition and mechanical properties of diamond-like carbon film using inert gases in methane plasma, Thin Solid Films 377-378, 198-202.

[4] Goujaro, S., Vandenbulcke, L., Tawil, H., (1994) the Oxidation Behaviour of Two-and Three-Dimensional C/SiC Thermostructural Materials Protected by Chemical-Vapour-Deposition Polylayers Coatings J. Mater. Sci. **29**, 6212-6220.

[5] R. E. Shroder, R. J. Nemanich & J. T. Glass, (1990) Analysis of the Composite Structures in Diamond Thin Films by Raman Spectroscopy, Phys. Rev. B **41**, 3738-3748

[6] A. C. Ferrari & J. Robertson, (2000) Interpretation of Raman Spectra of Disordered and Amorphous Carbon," Phys. Rev. B **61**, 14095-14017

[7] C. Casiraghi, A. C. Ferrari & J. Robertson, (2005) Raman Spectroscopy of Hydrogenated Amorphous Carbon, Phys. Rev. B **72**, 085401-085411.

[8] G. Adamopoulos, J. Robertson, N. A. Morrison & C. Godet, (2004) Hydrogen Content Estimation of Hydrogenated Amorphous Carbon by Visible Raman Spectroscopy, J. Appl. Phys. **96**, 6348 -6358.

[9] K. Miura, M. Nakamura, (2008) Analysis of Hydrogen Concentration in DLC Films by Raman Spectroscopy", J. Surf. Fin. Soc. Japan **59**, 203-205.

[10] J. Choi, T. Hibi, A. Furuno, M. Kawaguchi, T. Kato, (2017) Evaluation and Prediction of Mechanical Properties of DLC Films by Raman Spectroscopy (Part 2), J. Japanese Soc. Tribol. **62**, 228-235.

[11] J. Roberston, (2002) Diamond-Like Amorphous Carbon, Mater. Sci. Eng. R: Rep. **37**, 129-281.

[12] G. G. Stoney, (1909) the Tension of Metallic Films Deposited by Electrolysis", Proceedings of the Royal Society of London, Series A **82**, 172-175.

[13] M. Nakamura, K. Miura, T. Matsuoka and T. Hirayama, (2008) Effects of Deposition Conditions on Residual Stress in DLC films Prepared by UBM Sputtering, J. JSMS **57**, 488-494.

[14] H. Kobayashi, Fracture mechanics, 10th Press, Kyoritsu Publishing Co., Ltd., Japan, 2005, 61-63.

[15] S. Takezono, Foundation strength of materials, 19th Press, Asakusa Shoten, Japan, 2002, 134-135.